








BRIEF ARTICLE

Test-Retest Variability of Relative Tracer Delivery Rate as Measured by [¹¹C]PiB

Fiona Heeman ¹, Janine Hendriks,¹ Isadora Lopes Alves ¹, Nelleke Tolboom ²,
 Bart N. M. van Berckel,¹ Maqsood Yaqub ¹, Adriaan A. Lammertsma ¹

¹Amsterdam UMC, Vrije Universiteit Amsterdam, Radiology and Nuclear Medicine, Amsterdam Neuroscience, De Boelelaan 1117, Amsterdam, The Netherlands

²Imaging Division, Department of Radiology, University Medical Center Utrecht, Utrecht, Netherlands

Abstract

Purpose: Moderate-to-high correlations have been reported between the [¹¹C]PiB PET-derived relative tracer delivery rate R_1 and relative CBF as measured using [¹⁵O]H₂O PET, supporting its use as a proxy of relative CBF. As longitudinal PET studies become more common for measuring treatment efficacy or disease progression, it is important to know the intrinsic variability of R_1 . The purpose of the present study was to determine this through a retrospective data analysis.

Procedures: Test-retest data belonging to twelve participants, who underwent two 90 min [¹¹C]PiB PET scans, were retrospectively included. The voxel-based implementation of the two-step simplified reference tissue model with cerebellar grey matter as reference tissue was used to compute R_1 images. Next, test-retest variability was calculated, and test and retest R_1 measures were compared using linear mixed effect models and a Bland-Altman analysis.

Results: Test-retest variability was low across regions (max. 5.8 %), and test and retest measures showed high, significant correlations ($R^2=0.92$, slope=0.98) and a negligible bias (0.69 ± 3.07 %).

Conclusions: In conclusion, the high precision of [¹¹C]PiB R_1 suggests suitable applicability for cross-sectional and longitudinal studies.

Key words: [¹¹C]PiB, Alzheimer's disease, Cerebral blood flow, Relative tracer delivery, Test-retest variability

Background

Cerebral blood flow (CBF) is known to decline with age, and elderly individuals (75–80 years) may present with reductions in CBF of up to 25 % compared with young adults (± 25 years) [1, 2]. In the context of Alzheimer's disease (AD), additional reductions in CBF have been reported in several cortical brain regions such as the frontal, parietal and temporal cortices with both absolute reductions as well as relative to cerebellar grey matter reference tissue

[3, 4]. This pattern of CBF reductions is considered characteristic of AD pathology and may therefore be used as proxy for measuring disease severity or progression [5, 6]. The gold standard technique for measuring CBF is [¹⁵O]H₂O positron emission tomography (PET) [7], but MR-based techniques such as arterial spin labelling (ASL) have also been introduced [5]. More recently, several studies have evaluated whether a valid proxy of cerebral perfusion can be obtained from the early frames of dynamic scans using currently available PET tracers (e.g. for measuring amyloid- β or tau burden) [3, 8]. The relative influx rate ($R_1=K_1/K_1'$), which can be calculated from these early frames, is an indirect measure of relative CBF as it is also

Correspondence to: Fiona Heeman; e-mail: f.heeman@amsterdamumc.nl

affected by the extraction fraction ($K_1=E \cdot CBF$). In particular, for the amyloid tracer [¹¹C]PiB, Chen and colleagues have reported that in cortical regions, relative tracer delivery R_1 showed moderate-to-high correlations with relative CBF measured using dynamic [¹⁵O]H₂O PET (with a range of $\rho=0.68-0.84$, $p<0.001$, across cortical regions and a value of $\rho=0.82$, $p<0.001$, for the global cortical region), thereby indicating that [¹¹C]PiB could be used for dual-biomarker imaging [9]. Furthermore, Bilgel and colleagues demonstrated that in a longitudinal setting with an average follow-up duration of 2.5 years, rates of change as measured with R_1 showed low-to-moderate correlations with changes in [¹⁵O]H₂O PET CBF (median $r=0.42$ across cortical regions and a value of $r=0.65$ for the global cortical region). In addition, rates of change as measured with R_1 required the smallest sample-size for detecting group-wise differences (27 % reduction compared with [¹⁵O]H₂O PET), suggesting this proxy could be suitable for tracking long-term longitudinal changes in CBF [8]. As longitudinal PET studies in AD become more common for measuring treatment efficacy or disease progression, it is important to know the intrinsic variability of R_1 in order to determine what magnitude of change in R_1 signifies an actual change. Therefore, the purpose of the present retrospective analysis of a previously reported test-retest (TRT) [¹¹C]PiB study was to assess the precision of [¹¹C]PiB R_1 .

Materials and Methods

Subjects

Data from twelve participants belonging to a TRT study conducted within the Amsterdam UMC, location VUmc, were reanalysed as the original study only reported TRT variability for the non-displaceable binding potential [10]. This dataset consisted of five cognitively unimpaired (CU) subjects, one patient with mild cognitive impairment (MCI) and six with AD dementia, which in the present study was used to examine TRT variability for R_1 [10]. Before enrolment, written informed consent was obtained from all individual participants included in the study, and the Medical Ethics Review Committee of the Amsterdam UMC, location VUmc, had approved the study.

Image Acquisition

All subjects underwent a structural T1-weighted MR scan on a 1.5T Siemens Sonata scanner and, within 1 week, two 90-min dynamic [¹¹C]PiB PET scans (test and retest) on a Siemens ECAT EXACT HR+ scanner [10]. Each dynamic scan consisted of 23 consecutive time frames (1×15, 3×5, 3×10, 2×30, 3×60, 2×150, 2×300, 7×600 s). All participants received an intravenous injection of, on average 332 ±70 MBq for test (353±26 for CUs, 138 for the MCI patient, and 342±66 for the AD dementia patients) and 376

±43 MBq (355±37 for CUs, 368 for the MCI patient, and 393±47 for the AD dementia patients) for retest scans.

Image Processing

Structural T1-weighted MR images were co-registered to their corresponding PET image segmented into grey matter (GM), white matter (WM) and cerebrospinal fluid (CSF) using PVE-lab software [11]. Next, volumes of interest (VOIs) were delineated based on the Hammers atlas and a reference tissue time-activity curve (TAC) of the cerebellar grey matter was extracted [12, 13].

Parametric Analysis

The PPET software tool [14] with the voxel-based implementation of the two-step simplified reference tissue model (SRTM2), as validated for [¹¹C]PiB, and cerebellar grey matter as reference tissue were used to compute relative tracer delivery (R_1) images [15–17]. For SRTM2, k_2' was determined across all voxels with a BP_{ND} higher than 0.05 by taking the median k_2' from a first run using receptor parametric mapping (RPM) [18]. Regional R_1 values were obtained by superimposing the following grey matter VOIs on the parametric images: medial and lateral anterior temporal lobe, posterior temporal lobe, superior, middle and inferior temporal gyrus, fusiform gyrus, parahippocampal and ambient gyrus, anterior and posterior cingulate gyrus, middle and orbitofrontal gyrus, gyrus rectus, inferior and superior frontal gyrus, pre- and post-central gyrus, superior parietal gyrus and the (infero)lateral remainder of the parietal lobe and a global cortical composite region (i.e. volume-weighted average across all target regions).

Statistical Analysis

Statistical analyses were performed in R (version 4.0.3; R Foundation for Statistical Computing, Vienna, Austria). First, global R_1 values were compared between CU and AD dementia groups using a non-parametric Mann-Whitney U test, separately for test and retest scans. Next, TRT variability was calculated for regional and global cortical R_1 values according to Eq. 1, where T represents the estimate of R_1 measured during test, and R the one measured during retest.

$$TrT \text{ variability } (\%) = \frac{|T-R|}{0.5 \cdot |T+R|} \cdot 100 \quad (1)$$

In addition, a correlation analysis was used to assess the relationship between TRT variability and regional volume.

Furthermore, to assess the relationship between test and retest R_1 measures, linear mixed effect models (LME) were fitted and correlation coefficients were calculated using the nlme and MuMIn packages, respectively [19, 20]. Visual read (amyloid- β positive or negative) was used as a covariate and the analysis accounted for the within-subject correlation between regions. Finally, a Bland-Altman analysis was used to assess potential bias between test and retest R_1 using the blandr package [21, 22].

Results

Participant characteristics are shown in Table 1. Relative tracer delivery measures (R_1) are reported in Table 2, with a significantly lower global R_1 in AD dementia patients compared with CU participants, for both test and retest scans ($p < 0.01$).

Regional and global cortical TRT variability values are presented in Table 3. TRT variability for the global cortical composite was low (1.70 %), while the range of regional TRT variability showed slightly higher values (range: 1.52–5.78 %). Furthermore, there was a trend effect towards smaller TRT variability for larger regions ($R^2=0.14$, $p=0.09$).

LME analyses showed that test and retest R_1 values were strongly correlated and that the slope was not significantly different from 1 ($R^2=0.92$, slope=0.98 C.I. [0.94–1.01], $p<0.001$). Furthermore, amyloid status as measured by visual read did not have a significant effect on this relationship. Finally, Bland-Altman analysis showed a negligible bias (0.69±3.07 %) between test and retest R_1 (Fig. 1). All analyses were also carried out using RPM-derived R_1 which resulted in essentially identical results (data not shown).

Discussion

The present study assessed precision of the R_1 parameter, a measure of relative tracer delivery, through a retrospective analysis of a previously reported [¹¹C]PiB test-retest study [11]. Low test-retest variability was observed for SRTM2-derived R_1 , and this was true for regions of different sizes.

Differences in R_1 between diagnostic groups were as expected, with lower average R_1 values in AD dementia patients compared with CU participants. This finding is in agreement with existing literature where decreases in

Table 1 Subject demographics

	CU (N= 5)	MCI (N=1)	AD dementia (N=6)
Age	64.6 ±6.4	71.0	61.0 ±3.0
Females	60 %	100 %	17 %
VR positive	20 %	0 %	100 %
MMSE	29.8 ±0.4	28.0	20.7 ±2.0

VR visual read, MMSE mini mental state examination
Values are depicted as mean±SD, unless indicated otherwise

Table 2 Relative tracer delivery values by diagnostic group

Diagnostic groups	SRTM2-derived R_1	
	Test	Retest
CU (N=5)	0.93 ± 0.04	0.91 ± 0.03
MCI (N=1)	0.91	0.91
AD dementia (N=6)	0.82 ± 0.04	0.82 ± 0.03

Values are depicted as mean±SD

(relative) perfusion related to AD pathology have been reported for both R_1 and [¹⁵O]H₂O PET studies [3, 23, 24]. Furthermore, by incorporating these two groups, the present study covered the entire range of R_1 values that would be expected in clinical studies across the AD spectrum.

Excellent TRT variability was observed for the global cortical composite (1.70 %) and only a slightly poorer TRT variability for some of the smaller regions (max 5.8 %). These findings were supported by the results of the LME analysis which showed a high correlation between test and retest R_1 measures ($R^2=0.92$) and a slope that was close to identity. As expected, the results indicate that smaller TRT variability was associated with larger regions. This finding suggests that studies should consider looking at relatively larger regions with PET when their aim is to detect small (<5 %) changes. Despite distinct kinetics, the present findings were also comparable with results from a [¹⁸F]florbetapir study that assessed TRT variability of SRTM-derived R_1 in a very similar population in terms of age and diagnosis (max. TRT variability of 6 %) [25]. Comparing [¹¹C]PiB R_1 TRT variability with TRT variability of absolute perfusion as

Table 3 Regional test-retest variability (%) of R_1

Region*	SRTM2-derived R_1
Global Cortex	1.70
Anterior temporal lobe medial part	2.77
Anterior temporal lobe lateral part	2.48
Parahippocampal and ambient gyri	3.02
Superior temporal gyrus	2.68
Middle and inferior temporal gyri	2.87
Fusiform gyrus	2.26
Insula	2.06
Lateral remainder of occipital lobe	2.08
Gyrus cinguli anterior part	1.52
Gyrus cinguli posterior part	3.44
Middle frontal gyrus	2.13
Posterior temporal lobe	2.11
Inferolateral remainder of parietal lobe	2.31
Precentral gyrus	1.71
Gyrus rectus	5.78
Orbitofrontal gyri	3.06
Inferior frontal gyrus	2.00
Superior frontal gyrus	2.08
Postcentral gyrus	1.79
Superior parietal gyrus	1.59
Lingual gyrus	2.60
Cuneus	1.76

*All values are average % TRT variability across N=11 subjects

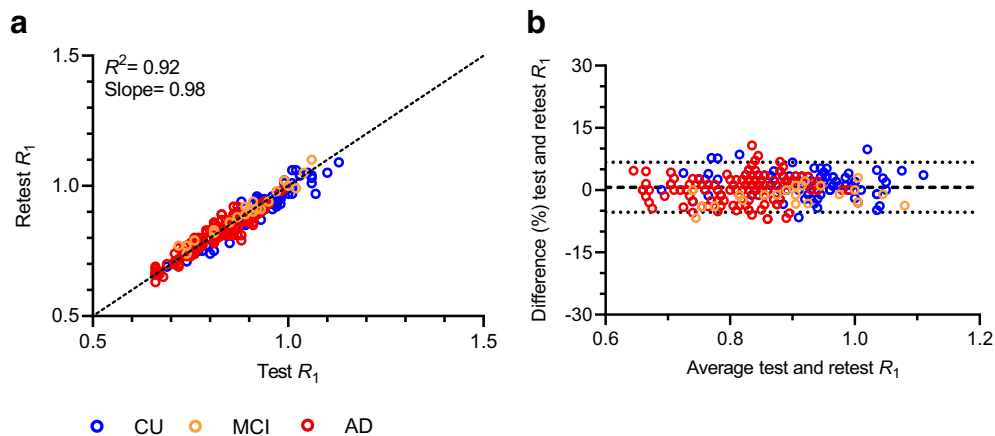


Fig. 1. Relationship between SRTM2-derived test and retest R_1 . (a) The correlation between R_1 test and retest measures, with R^2 and slope parameters corresponding to the LME analysis and (b) a Bland-Altman plot, which indicates the bias between the two measures.

measured with the gold-standard, [^{15}O]H $_2$ O PET [26], shows that the present results are slightly better, indicating that R_1 is a more precise measure likely due to the fact that it is a relative measure. Furthermore, given that R_1 is an indirect measure of perfusion, variation in the extraction fraction may compensate day-to-day fluctuations in flow to maintain constant delivery. On the other hand, this also means that alterations in extraction fraction may bias R_1 , as opposed to the gold standard [^{15}O]H $_2$ O PET which provides a direct measurement of CBF. Unfortunately, to date, no studies have reported TRT variability of relative perfusion as measured with [^{15}O]H $_2$ O PET with cerebellar grey matter reference tissue for a direct comparison. Nonetheless, a study by Bilgel and colleagues compared long-term variability of CBF proxies (i.e. [^{11}C]PiB PET-derived R_1 and early frame standardised uptake value ratios) to that of [^{15}O]H $_2$ O PET and reported that, across these three measures, the highest longitudinal stability was obtained with R_1 . The present study demonstrates that R_1 also has low short-term variability. Therefore, R_1 could be considered a valid alternative to measuring longitudinal changes in CBF, thereby circumventing the need for a separate [^{15}O]H $_2$ O PET scan. Unfortunately, it remains unclear whether changes across a lifetime are comparable between R_1 and rCBF as measured by [^{15}O]H $_2$ O PET. One study reports that, in an elderly population (77 \pm 8 years old), the yearly percentage change in R_1 was lower (-0.28 %) than that in regional CBF (-0.41 %) as measured by [^{15}O]H $_2$ O PET, although it was not reported whether this difference was significant [8]. Nevertheless, a smaller change in R_1 , especially in elderly subjects, may be related to an increased extraction fraction [27]. However, longitudinal studies of R_1 in a younger population are needed to confirm whether the same difference is present earlier in life. Furthermore, using a relative parameter to measure CBF such as R_1 essentially assumes that there are no CBF changes in the reference tissue ($R_1=K_1/K_1'$). In this regard, it should be noted that

differences in whole cerebellum CBF (a commonly used reference tissue) have been reported when comparing AD dementia patients and age-matched controls [28]. In contrast, such differences have not been demonstrated for cerebellar cortex CBF by studies using a similar design in terms of technique and participants [24, 29–31]. This suggests that careful interpretation is required when comparing longitudinal R_1 measurement between AD dementia patients and controls or that alternative reference tissues, unaffected by CBF changes, should be considered. Yet, further research is required to understand whether such changes in cerebellar CBF also occur in early AD stages.

Conclusion

Relative tracer delivery rate R_1 of [^{11}C]PiB showed high global and regional precision in participants covering the AD spectrum. Therefore, [^{11}C]PiB R_1 appears to be a stable parameter for measuring cross-sectional differences and longitudinal changes in relative CBF.

Author Contribution. FH, JH, MY, ILA, AAL contributed to the study design, analyses, data interpretation and drafting of the manuscript. NT and BvB contributed to data acquisition. All authors critically reviewed, and approved the final version of the work.

Funding. This project received funding from the EU/EFPIA Innovative Medicines Initiative (IMI) Joint Undertaking (EMIF grant 115372) and the EU-EFPIA IMI-2 Joint Undertaking (grant 115952). This joint undertaking receives support from the European Union's Horizon 2020 research and innovation program and EFPIA. This communication reflects the views of the authors and neither IMI nor the European Union and EFPIA are liable for any use that may be made of the information contained herein.

Declarations

Ethical Approval

All procedures performed in studies involving human participants were in accordance with the ethical standards of the institutional and/or national

research committee and with the 1964 Helsinki declaration and its later amendments or comparable ethical standards.

Conflict of Interest

The authors declare that they have no conflict of interest.

Open Access This article is licensed under a Creative Commons Attribution 4.0 International License, which permits use, sharing, adaptation, distribution and reproduction in any medium or format, as long as you give appropriate credit to the original author(s) and the source, provide a link to the Creative Commons licence, and indicate if changes were made. The images or other third party material in this article are included in the article's Creative Commons licence, unless indicated otherwise in a credit line to the material. If material is not included in the article's Creative Commons licence and your intended use is not permitted by statutory regulation or exceeds the permitted use, you will need to obtain permission directly from the copyright holder. To view a copy of this licence, visit <http://creativecommons.org/licenses/by/4.0/>.

References

- Pantano P, Baron JC, Lebrun-Grandié P, Duquesnoy N, Bousser MG, Comar D (1984) Regional cerebral blood flow and oxygen consumption in human aging. *Stroke*. 15:635–641
- Leenders KL, Perani D, Lammertsma AA, Heather JD, Buckingham P, Healy MJ et al (1990) Cerebral blood flow, blood volume and oxygen utilization. Normal values and effect of age. *Brain*. 113(Pt 1):27–47
- Ottoy J, Verhaeghe J, Niemantsverdriet E, De Roock E (2019) wyffels L, Ceysens S, et al. 18F-FDG PET, the early phases and the delivery rate of 18F-AV45 PET as proxies of cerebral blood flow in Alzheimer's disease: Validation against 15O-H₂O PET. *Alzheimers Dement* 15:1172–1182
- Fukuyama H, Ogawa M, Yamauchi H, Yamaguchi S, Kimura J, Yonekura Y et al (1994) Altered cerebral energy metabolism in Alzheimer's disease: a PET study. *J Nucl Med Soc Nucl Med* 35:1–6
- Collij LE, Heeman F, Kuijter JPA, Ossenkoppel R, Benedictus MR, Möller C, Verfaillie SCJ, Sanz-Arigita EJ, van Berckel BNM, van der Flier WM, Scheltens P, Barkhof F, Wink AM (2016) Application of machine learning to arterial spin labeling in mild cognitive impairment and Alzheimer disease. *Radiology*. 281:865–875
- Wierenga CE, Hays CC, Zlatar ZZ (2014) Cerebral blood flow measured by arterial spin labeling MRI as a preclinical marker of Alzheimer's disease. *J Alzheimers Dis* 42:S411–S419
- Jagust WJ, Eberling JL, Reed BR, Mathis CA, Budinger TF (1997) Clinical studies of cerebral blood flow in Alzheimer's disease. *Ann N Y Acad Sci* 826:254–262
- Bilgel M, Beason-Held L, An Y, Zhou Y, Wong DF, Resnick SM (2020) Longitudinal evaluation of surrogates of regional cerebral blood flow computed from dynamic amyloid PET imaging. *J Cereb Blood Flow Metab* 40:288–297
- Chen YJ, Rosario BL, Mowrey W, Laymon CM, Lu X, Lopez OL, Klunk WE, Lopresti BJ, Mathis CA, Price JC (2015) Relative 11C-PiB delivery as a proxy of relative CBF: quantitative evaluation using single-session 15O-water and 11C-PiB PET. *J Nucl Med* 56:1199–1205
- Tolboom N, Yaqub M, Boellaard R, Luurtsema G, Windhorst AD, Scheltens P, Lammertsma AA, van Berckel BNM (2009) Test-retest variability of quantitative [11C]PiB studies in Alzheimer's disease. *Eur J Nucl Med Mol Imaging* 36:1629–1638
- Rask T, Dyrby T, Comerci M, Alfano B, Quarantelli M, Berkouk K et al (2004) PVElab: Software for correction of functional images for partial volume errors. *Neuroimage*. 22
- Hammers A, Allom R, Koeppe MJ, Free SL, Myers R, Lemieux L, Mitchell TN, Brooks DJ, Duncan JS (2003) Three-dimensional maximum probability atlas of the human brain, with particular reference to the temporal lobe. *Hum Brain Mapp* 19:224–247
- Heeman F, Hendriks J, Lopes Alves I, Ossenkoppel R, Tolboom N, van Berckel BNM et al (2020) [11C]PiB amyloid quantification: effect of reference region selection. *EJNMMI. Research*. 10:123
- Boellaard R, Yaqub M, Lubberink M, Lammertsma A (2006) PPET: A software tool for kinetic and parametric analyses of dynamic PET studies. *NeuroImage Supplement* 2:T62
- Wu Y, Carson RE (2002) Noise reduction in the simplified reference tissue model for neuroreceptor functional imaging. *J Cereb Blood Flow Metab* 22:1440–1452
- Yaqub M, Tolboom N, Boellaard R, van Berckel BNM, van Tilburg EW, Luurtsema G, Scheltens P, Lammertsma AA (2008) Simplified parametric methods for [11C]PiB studies. *Neuroimage*. 42:76–86
- Peretti DE, Vázquez García D, Reesink FE, van der Goot T, De Deyn PP, de Jong BM et al (2019) Relative cerebral flow from dynamic PiB scans as an alternative for FDG scans in Alzheimer's disease PET studies. *PLoS One* 14:e0211000
- Gunn RN, Lammertsma AA, Hume SP, Cunningham VJ (1997) Parametric imaging of ligand-receptor binding in PET using a simplified reference region model. *NeuroImage*. 6:279–287
- Pinheiro J, Bates D, DebRoy S, Sarkar D, R Core Team. nlme: linear and nonlinear mixed effects models. 2021. Available from: <https://CRAN.R-project.org/package=nlme>
- Barton K. MuMIn: Multi-Model Inference. 2020. Available from: <https://CRAN.R-project.org/package=MuMIn>
- Datta D. blandr: a Bland-Altman method comparison package for R. Zenodo; 2017. Available from: <https://zenodo.org/record/824514>
- Martin Bland J (1986) Altman DouglasG. Statistical methods for assessing agreement between two methods of clinical measurement. *Lancet* 327:307–310
- Deo AK, Borson S, Link JM, Domino K, Eary JF, Ke B, Richards TL, Mankoff DA, Minoshima S, O'Sullivan F, Eyal S, Hsiao P, Maravilla K, Unadkat JD (2014) Activity of P-glycoprotein, a β-amyloid transporter at the blood-brain barrier, is compromised in patients with mild Alzheimer's disease. *J Nucl Med* 55:1106–1111
- Ishii K, Sasaki M, Yamaji S, Sakamoto S, Kitagaki H, Mori E (1998) Paradoxical hippocampus perfusion in mild-to-moderate Alzheimer's disease. *J Nucl Med* 39:293–298
- Golla SS, Verfaillie SC, Boellaard R, Adriaanse SM, Zwan MD, Schuit RC et al (2018) Quantification of [18F]florbetapir: A test-retest tracer kinetic modelling study. *J Cereb Blood Flow Metab* 39:2172–2180
- Bremmer JP, van Berckel BNM, Persoon S, Kappelle LJ, Lammertsma AA, Kloet R, Luurtsema G, Rijbroek A, Klijn CJM, Boellaard R (2011) Day-to-day test-retest variability of CBF, CMRO₂, and OEF measurements using dynamic 15O PET studies. *Mol Imaging Biol* 13:759–768
- van Assema DME, Lubberink M, Boellaard R, Schuit RC, Windhorst AD, Scheltens P, Lammertsma AA, van Berckel BNM (2012) P-glycoprotein function at the blood-brain barrier: effects of age and gender. *Mol Imaging Biol* 14:771–776
- Kuwabara Y, Ichiya Y, Otsuka M, Masuda K, Ichimiya A, Fujishima M (1992) Cerebrovascular responsiveness to hypercapnia in Alzheimer's dementia and vascular dementia of the Binswanger type. *Stroke*. 23:594–598
- Ishii K, Sasaki M, Matsui M, Sakamoto S, Yamaji S, Hayashi N, Mori T, Kitagaki H, Hirono N, Mori E (2000) A diagnostic method for suspected Alzheimer's disease using H(2)15O positron emission tomography perfusion Z score. *Neuroradiology*. 42:787–794
- Cohen RM, Andreason PJ, Doudet DJ, Carson RE, Sunderland T (1997) Opiate receptor avidity and cerebral blood flow in Alzheimer's disease. *J Neuro Sci* 148:171–180
- Ottoy J, Verhaeghe J, Niemantsverdriet E, Wyffels L, Somers C, Roock ED et al (2017) Validation of the semiquantitative static SUVR method for 18F-AV45 PET by pharmacokinetic modeling with an arterial input function. *J Nucl Med* 58:1483–1489

Publisher's Note. Springer Nature remains neutral with regard to jurisdictional claims in published maps and institutional affiliations.